

δ -Toxin and Analogues as Peptide Models for Protein Ion Channels

Christine M. Bladon,^{a*} Peter Bladon^b and John A. Parkinson^a

^a Department of Chemistry, University of Edinburgh, West Mains Road, Edinburgh EH9 3JJ, UK

^b Department of Pure and Applied Chemistry, University of Strathclyde, 295 Cathedral Street, Glasgow G1 1XL, UK

δ -Toxin, six analogues and their acetylated derivatives, have been synthesised. The model peptides, based on the parent compound δ -toxin, incorporate components of the proposed pore-forming segments of the protein ion channels. The backbone conformations of the peptides have been elucidated by a combination of two-dimensional NMR experiments and distance geometry and molecular mechanics calculations. In several of the compounds a relatively stable helix is formed but in peptides incorporating a proline in the centre of the molecule a bend-helix motif is present.

Ion channels are proteins which control the flow of ions across biological membranes. The channels are highly selective—some ions are permitted to pass but not others. The proteins which form the various K^+ , Na^+ and Ca^{2+} channels have a similar structure—they are composed of subunits of α -helices that associate in a tetrameric arrangement to form the ion-conducting pore. This aqueous pore through which the ions pass is shaped rather like an hourglass with wide entrances which narrow to a restrictive region. It is this constriction of the pore diameter together with binding sites which are responsible for the ionic selectivity.¹ One of the α -helical regions of the proteins, segment 2 (S2), has been proposed as the pore-forming sequence² although a number of other models involving different regions have also been suggested.³ The amino acid sequence of the S2 segments differ, although there are similarities both between subunits within a given protein and between equivalent subunits of different proteins. The S2 segments are amphiphilic and the charged amino acids are conserved. At equivalent positions in each of the four subunits a glutamic acid and a lysine residue on the same side of the α -helix are conserved and two of the subunits have an additional acidic amino acid located 10 residues from that glutamic acid on the same side of the α -helix. An aromatic amino acid also occurs in each S2 segment in similar positions. In a system this complex, involving four similar but different sequences, it is difficult to determine which residues are critical in determining ionic selectivity and precisely where they are located.

A number of naturally occurring amphiphilic peptides,⁴ e.g. mellitin,⁵ alamethicin⁶ and paradaxin⁷ and synthetic peptides^{8,9} have been reported to form ion channels. δ -Toxin (Fig. 1) is a 26 amino acid peptide from *Staphylococcus aureus* which can adopt an amphiphilic structure and forms cation channels consisting of a hexameric cluster of molecules.¹⁰ Furthermore, the primary sequence of this peptide bears important similarities to the S2 segments of the protein channels. When δ -toxin and the S2 segments are aligned (Table 1) an acidic (Asp¹⁸), a basic (Lys²²) and an aromatic (Trp¹⁵) amino acid occur in similar positions to those present in the protein segments. The amphiphilic nature of δ -toxin and its ability to form cation channels together with its similarity to the S2 segments made this peptide a suitable choice to try and model the narrow region of the ion channel pore. A number of peptides were designed, based on δ -toxin but incorporating components of the S2 sequences, which are simple enough to facilitate structural interpretation of their channel forming properties.

This paper describes the synthesis and structural investigation of the series of model peptides. The parent compound, δ -

toxin, and six analogues were prepared. Three types of modification were made (see Table 2): (1) A glutamic acid replaces either the threonine or serine at positions 8 or 7 respectively to give compounds 2 and 3. As alluded to earlier, two of the four S2 segments feature an acidic residue towards the *N*-terminus of the sequence. (2) A proline replaces the lysine at position 14 to yield compound 4. Proline is known to kink helices¹⁶ and so in a cluster of molecules which form a channel this may have the effect of narrowing the pore. (3) Omission of the lysine at position 14 to give compound 5. When this charged amino acid is left out, the non-polar residues of Leu¹² and Val¹³ are immediately followed by the aromatic amino acid which is a situation more akin to the S2 segments. A helical wheel projection of this peptide still indicates an amphiphilic helix.

In addition to these single amino acid changes, two peptides were synthesised which featured a combination of these modifications—namely Glu⁸, Pro¹⁴- δ -toxin 6 and Glu⁷, des-Lys¹⁴- δ -toxin 7. The *N*-acetylated derivatives of each of seven peptides was also prepared (1a–7a). The *N*-terminus of δ -toxin is probably not the free amine but is blocked with a formyl group. Although the presence or absence of a blocking group was not expected to noticeably affect the structure of the peptide, acetylation may enhance the dipolarity of the peptide and favour alignment in the electric field. These acetylated derivatives were thus prepared largely for the biological studies.

NMR studies on the conformation of natural bacterial δ -toxin have been reported. In methanol, δ -toxin adopts a helical structure¹⁷ extending from Ala² to Val²⁰. When bound to phospholipid micelles (an artificial membrane environment) a similar structure was observed¹⁸ although in this case the helix was found to extend over a slightly different range—from residues 5 to 23. In our studies we elected to determine the structure of the synthetic peptides in methanol, or in a largely methanolic solution, as such a simple solvent system appeared to be a reasonable alternative to the more realistic but complex membrane environment.

δ -Toxin and the series of analogues were prepared using standard methods of solid-phase peptide synthesis. No significant problems were encountered during the chain assembly process. After cleavage of the final Fmoc group approximately one-quarter of the resin-bound peptide was acetylated by treatment with acetic anhydride. Analytical HPLC of the crude peptides immediately after cleavage from the resin indicated that, in each case, the required compound was the major product and that no significant impurities were present. Purification was straightforward. Traces of scavengers and low molecular weight material were removed by a gel-filtration

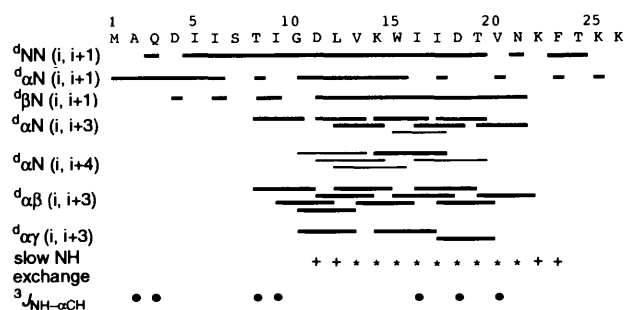


Fig. 2 Summary of inter-residue NMR spectroscopic data for δ -toxin in CD_3OH^*

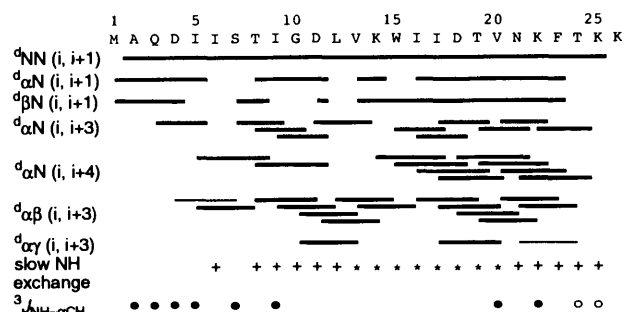


Fig. 3 Summary of inter-residue NMR spectroscopic data for δ -toxin in $CD_3OH-H_2O (2:1)^*$

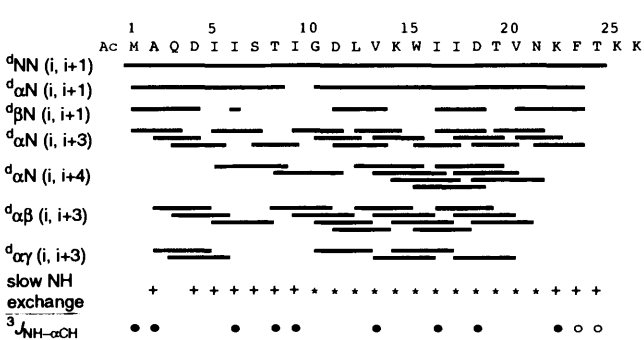


Fig. 4 Summary of inter-residue NMR spectroscopic data for Ac- δ -toxin in $CD_3OH-H_2O (2:1)^*$

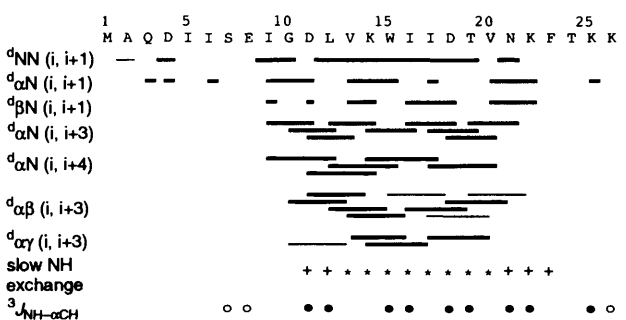


Fig. 5 Summary of inter-residue NMR spectroscopic data for Glu⁸- δ -toxin in CD_3OH^*

the ring protons of the phenylalanine as they were bunched within a 0.2 ppm range. The chemical shifts and assignments for all 26 residues of each peptide (25 residues for des-Lys¹⁴- δ -toxin) are listed in the Experimental section.

The NOESY was the pivotal experiment and provided the essential data for the structure determination. The NOESY off-diagonal cross peaks result from through-space interactions between protons of different amino acid residues separated by a distance of less than 5 Å. Using the sequential NOEs between

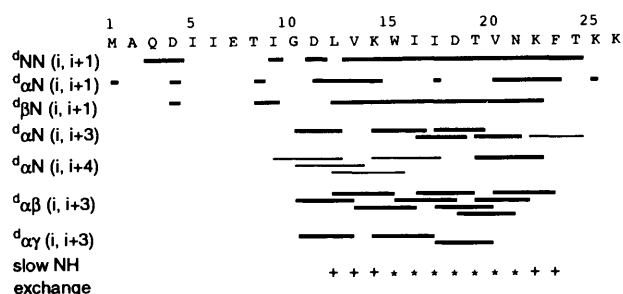


Fig. 6 Summary of inter-residue NMR spectroscopic data for Glu⁷- δ -toxin in CD_3OH^*

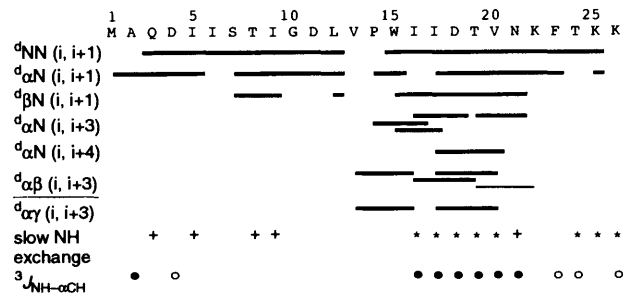


Fig. 7 Summary of inter-residue NMR spectroscopic data for Pro¹⁴- δ -toxin in CD_3OH^*



Fig. 8 Summary of inter-residue NMR spectroscopic data for des-Lys¹⁴- δ -toxin in $CD_3OH-H_2O (2:1)^*$

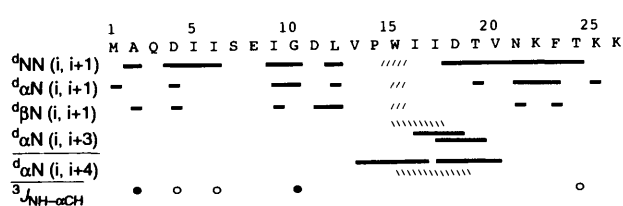


Fig. 9 Summary of inter-residue NMR spectroscopic data for Glu⁸, Pro¹⁴- δ -toxin in $CD_3OH-H_2O (2:1);$ // indicate the NOEs of the first conformation and // indicate the NOEs of the second conformation*

the αCH , βCH and the NH of one residue with the NH of the next residue (α_i-NH_{i+1} , β_i-NH_{i+1} and NH_i-NH_{i+1} respectively) it was possible to trace the connectivity along the backbone of each molecule and thus confirm the primary structure of the peptides (see first three rows of Figs. 2-9).*

* General comments for Figs. 2-9: Summary of the inter-residue NOE connectivities involving the NH, αCH , βCH and γCH protons. A line connects the two residues between which an NOE was observed. Thick bars indicate a strong NOE which was observed on both sides of the diagonal and thin bars indicate either a weak NOE or one which was only detected on one side of the diagonal. NH exchange: * indicate those protons still protonated after completion of the experiment and + indicate those amide protons which, although slow to exchange, were fully deuterated before completion of the experiment. $^3J_{NH-\alpha CH}$: full circles indicate a coupling constant < 6.0 Hz and open circles > 7.0 Hz.

peptides, most noticeably with Glu⁸, Pro¹⁴- δ -toxin **6**, connectivity was lost for short regions of the sequence. However, by comparison with more completely assigned spectra, *e.g.* δ -toxin and Ac- δ -toxin and on the basis of elimination, it was possible to tentatively assign particular residues to the various spin systems. For example, in Glu⁸, Pro¹⁴- δ -toxin, Ile⁵, Ile⁶ and Ile⁹ were assigned by sequential NOEs, thus leaving only isoleucines in positions 16 and 17 to be uniquely identified. In each of the other peptides studied, the α CH resonance of Ile¹⁶ was always slightly downfield from that of Ile¹⁷. Thus Ile¹⁶ and Ile¹⁷ of **6** were tentatively assigned based on this assumption (later confirmed by long range NOEs).

In addition to these NOEs between neighbouring amino acid residues, there were also a considerable number of α_i -NH_{*i*+3}, α_i -NH_{*i*+4}, α_i - β_{i+3} and α_i - γ_{i+3} NOEs *i.e.* interactions between non-adjacent residues (see rows 4–7 of Figs. 2–9). These long range NOEs are characteristic of secondary structure elements. In an α -helix there are 3.6 amino acids per turn of helix and consequently the distances between protons in the first amino acid residue to those of the third or fourth residue are within the range 0–5 Å, for which NOEs can be observed. In contrast, the proton–proton distances between residues 1 and 3 or 4 in an extended chain such as in a β -sheet conformation, are too long to be observed by the NOE effect. Analysis of the NOESY data clearly revealed a distinct α -helical region in each of the peptides studied by NMR spectroscopy.

The structure of δ -toxin **1** was studied in neat CD₃OH and in a CD₃OH–H₂O (2:1) solution. In methanol, a substantial number of long range NOEs were observed in the central portion of the molecule and extending towards the C-terminus (see Fig. 2). The α_i -NH_{*i*+4} NOEs are particularly significant as these are unique to the α -helix. The less common _{3,10} helix is a tighter structure and is characterised by α_i -NH_{*i*+2} interactions, and none of these were observed in δ -toxin. Thus in CD₃OH, δ -toxin adopts an α -helical structure between residues Thr⁸ and Lys²² with the terminal regions particularly the N-terminus, being relatively flexible. This conclusion was supported by two other parameters—small vicinal spin–spin coupling constants ³*J*_{NH- α CH} and slow amide–proton exchange data.

The size of ³*J*_{NH- α CH} is related to the intervening dihedral angle φ by the Karplus equation and small coupling constants (< 6 Hz) are characteristic of helical structure. Coupling constants were measured from the 1D spectrum but due to overlapping peaks only a few values could reliably be determined. Five residues—Thr⁸, Ile⁹, Ile¹⁶, Asp¹⁸ and Val²⁰—had small coupling constants (< 3.6 Hz) which supported the proposed α -helical region. Values for Ala² and Gln³ (*ca.* 4 and 5.1 Hz respectively) were also in the α -helical range and so conflicted to some extent with the NOE data.

Further independent evidence for an α -helical structure was provided by slow amide–proton exchange rates. In an α -helix there are hydrogen bonds of the type CO_{*i*}-NH_{*i*+4} and amide protons which exchange slowly with solvent thus identify the donor NH group of the hydrogen bond and the acceptor CO group is inferred. The NH protons of the first four residues of an α -helix are not involved in hydrogen bonds and are expected to exchange relatively quickly. Amide protons that were slow to exchange were identified by dissolving the peptide in deuterated solvent and recording 1D spectra over a period of time. In CD₃OD, the NH protons of Val¹³ to Asn²¹ of δ -toxin had not completely exchanged after 24 h, and those of residues 11, 12, 22 and 23 were observed for a time but had completely disappeared within 6 h. Unfortunately, several of the NH peaks overlapped in the 1D spectrum and so it was not possible to absolutely identify which resonance belonged to a particular residue. However, provided that there were several long range NOE interactions involving a particular residue it was assumed that the NH proton of that amino acid was slowly exchanging. Thus

the amide exchange data of δ -toxin supported the conclusion of an α -helical region in the centre of the molecule with extended conformations for the terminal segments.

Fig. 3 presents the survey of sequential NOEs, ³*J*_{NH- α CH} coupling constants, and NH exchange data for δ -toxin in the CD₃OH–H₂O (2:1) mixture. Numerous long range NOEs supported by NH exchange rates and a few coupling constants suggested that residues 5–24 formed an α -helix. The helical region possibly extended slightly further at either end; to Gln³ at the N-terminus and Lys²⁵ or Lys²⁶ at the C-terminus but the evidence was less convincing.

The third NMR study of δ -toxin (summarised in Fig. 4) was carried out with acetylated material in CD₃OH–H₂O (2:1). In this case there was conclusive evidence to show that the helical region extended over almost the entire length of the peptide. Again there were numerous NOEs characteristic of an α -helix in the central region but in addition there were strong interactions between the α CH of Met¹ and Ala² to appropriate NH protons further along the chain. Coupling constants for Met¹ and Ala² were both less than 6 Hz and confirmed that the helix extended to the N-terminus of the peptide. A lack of long range NOEs at the other end of the molecule together with large coupling constants for Phe²³ and Thr²⁴ (7.2 and 7.7 Hz respectively) indicated that the C-terminal tetrapeptide segment was unlikely to be helical. Finally, NH exchange data was compatible with the foregoing view that the α -helix spanned 22 residues from the N-terminus of the peptide to Lys²².

As a result of the helix dipole phenomenon a positive charge located near the N-terminus of a helix destabilises the structure.²⁰ Under the conditions of the NMR experiment the amine group at the N-terminus is protonated. This factor, combined with the dipole effect may account for the difference in the N-terminal limit of the α -helix in δ -toxin and Ac- δ -toxin. Furthermore, the solution structure of naturally occurring δ -toxin (N-formyl- δ -toxin) is virtually identical with that of Ac- δ -toxin and in both peptides the N-terminal amino group is effectively blocked. It is also interesting to note that the structure of the toxin obtained in CD₃OH–H₂O (2:1) is very similar to that reported for the natural material bound to phospholipid micelles.

The structures of the Glu⁸ **2** and Glu⁷ **3** analogues were determined in CD₃OH (see Figs. 5 and 6). Not unexpectedly, both compounds exhibited conformations similar to that of δ -toxin in CD₃OH. NOE and NH exchange data clearly indicated the presence of an α -helix between residues 8 or 9 and 22 or 23. Small ³*J*_{NH- α CH} couplings for a number of the residues within the 8–22 segment of the Glu⁸ analogue provided additional support for the helical structure. No values for ³*J*_{NH- α CH} were obtained for Glu⁷- δ -toxin.

Incorporation of a proline amino acid in the centre of the molecule had a pronounced effect on the structure. The long range NOE interactions (Fig. 7) of Pro¹⁴- δ -toxin **4** were confined to the C-terminal half of the peptide. An α -helical region extended from approximately the tryptophan at position 15 to the lysine at position 22. The C-terminal limit of the helix was reasonably clear cut, at residue 22, but the other end was less well-defined. Proline is a conformationally restricted amino acid and occupies a unique role in polypeptide structure. The fixed dihedral angles of proline residues induce disruption in helical structure at this amino acid but at the same time these angles are ideal for helix initiation. Thus in Pro¹⁴- δ -toxin it is probable that the proline residue is at the N-terminus of the α -helix and the preceding one or two residues form a bend. The interactions observed between the α CH of Val¹³ and the β and γ protons of Ile¹⁶ are therefore more likely to indicate that these residues are close in space due to a bend in the molecule rather than being incorporated into a helix. Further evidence for the short helix was obtained from coupling constant data. Six of the

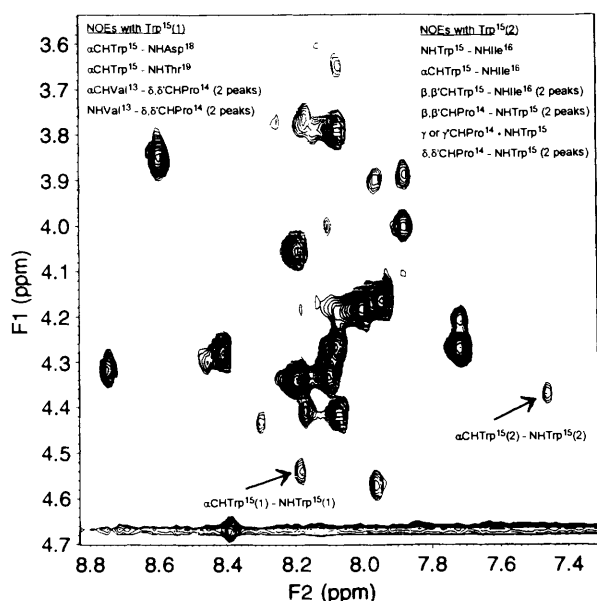


Fig. 10 TOCSY spectrum containing the $\alpha\text{CH-NH}$ cross peaks of Glu⁸, Pro¹⁴- δ -toxin **6**. Assignments of the peaks involving the two conformations are as indicated—labelled as Trp¹⁵(1) and Trp¹⁵(2). Inset are the inter-residue interactions, identified from the NOESY spectrum, involving the tryptophan residue.

eight residues exhibited small values for $^3J_{\text{NH-}\alpha\text{CH}}$. Moreover, these six residues formed the hexapeptide segment Ile¹⁶-Asn²¹ which is the core of the α -helix.

Omission of the residue at position 14 in δ -toxin caused surprisingly little effect on the overall structure of the molecule. The results of the des-Lys¹⁴- δ -toxin NMR experiments are summarised in Fig. 8. The combination of NOE, coupling constant and NH exchange data identified a helical region between approximately residue 7 and residue 22 of 5. Once again, the *N*- and *C*-terminal segments of the peptide were relatively unstructured.

The NMR spectra of Glu⁸, Pro¹⁴- δ -toxin were interesting but disappointing. Although the spectra of **6** were recorded as a dilute solution in CD₃OH-H₂O (2:1) the peptide aggregated and the NMR solution became very viscous after a few hours. However, several $\alpha_i\text{-NH}_{i+3}$ and $\alpha_i\text{-NH}_{i+4}$ NOEs were observed between residues 13 and 21 (see Fig. 9) but due to lack of resolution and poor signal to noise in the NOESY spectrum it was not possible to positively identify any $\alpha_i\text{-}\beta_{i+3}$ and $\alpha_i\text{-}\gamma_{i+3}$ interactions. Many of the NH resonances in the 1D spectrum were overlapped and consequently few $^3J_{\text{NH-}\alpha\text{CH}}$ coupling constants could be determined. Neither was it possible to establish the position of any hydrogen bonds. Although several NH protons were in slow exchange with the solvent the overlap problem prevented reliable NH assignments. Nevertheless, the pattern of the few long range NOEs suggested a structure for Glu⁸, Pro¹⁴- δ -toxin similar to that of the Pro¹⁴ analogue, *i.e.* a bend-helix motif in the centre of the molecule with flexible terminal segments.

The most interesting conformational feature of **6** was detected in the TOCSY spectrum. Two sets of cross peaks were observed for the NH and AMX spin system of Trp¹⁵ (Fig. 10). The chemical shifts of the NH protons differed by approximately 0.7 ppm. The lower chemical shift value (8.22 ppm), labelled Trp¹⁵(1), was similar to that observed for the NH proton of Trp¹⁵ in δ -toxin and several of the analogues. The position of the other NH resonance at 7.50 ppm [Trp¹⁵(2)] correlated well with that found for the NH protons of the tryptophan residue in Pro¹⁴- δ -toxin. The chemical shifts of the duplicate α and β protons were easily located although the βCH_2 resonances of

Trp¹⁵(1) were at a slightly lower frequency than expected. If the indole ring system was orientated perpendicular to the peptide backbone, the ring current effect would shield the NH proton and result in the observed shift to lower frequency of the NH resonance in Trp¹⁵(2). Thus, in the majority of the peptides studied and in one conformation of Glu⁸, Pro¹⁴- δ -toxin the side chain of tryptophan is projected away from the backbone. In Pro¹⁴- δ -toxin and in the second conformation of Glu⁸, Pro¹⁴- δ -toxin the indole ring is bent back towards the backbone of the peptide.

Long range NOEs were observed between the αCH of Trp¹⁵(1) and the NH protons of Asp¹⁸ and Thr¹⁹ (see inset in Fig. 10). Additional inter-residue NOEs were also detected between this αCH and NH protons of Val¹³ and the δ -protons of Pro¹⁴. In contrast, the protons of Trp¹⁵(2) were only involved in sequential NOEs to the adjacent Pro¹⁴ and Ile¹⁶ residues. Thus, it appeared likely that there were two distinct conformational families of Glu⁸, Pro¹⁴- δ -toxin possibly as a consequence of *cis-trans* isomerism about the Val¹³-Pro¹⁴ amide bond.

No substantial evidence was found for inter-chain interactions. The occasional cross peak in the NOESY spectrum of three of the compounds [δ -toxin (in CD₃OH) and the Glu⁷ and Glu⁸, Pro¹⁴ analogues] could be assigned to this type of interaction. If genuine, these dimers were formed from a head to tail association of the peptide chains.

The only remaining incongruous element from the NMR spectra was detected in the NH exchange experiment of Pro¹⁴- δ -toxin. In addition to the slow NH protons in the short helical segment there were a number of others which were also in slow exchange with the solvent. Several of these latter peaks were unambiguously assigned to amide protons in the relatively unstructured region of the peptide, in residues 3, 5, 8, 9, 24, 25 and 26. Thus in Pro¹⁴- δ -toxin there may be hydrogen bonds formed between the *C*-terminal segment of one molecule and the *N*-terminal segment of a second molecule.

Cross peaks due to interactions involving γ , δ and ϵ protons were also observed and assigned in the NOESY spectrum of each compound (see Table 3 under miscellaneous inter-residue interactions). These additional NOEs were not included in the input for the structure determination.

Structures based on the NMR data were calculated using the distance geometry program DGEOM.²¹ This works by generating structures which satisfy constraints on distances between pairs of atoms and torsional angle constraints between sets of atoms. A starting structure is modified by alterations in torsional angles while keeping the bond lengths and bond angles constant. The overall result is a family of conformers and each conformation within a family represents a solution to the problem of fitting the peptide chain to all the experimental constraints. The structures were further refined with the molecular mechanics program PIFF²² using the same set of constraints. Generated structures were displayed, analysed and manipulated using INTERCHEM²³ graphics. All calculations were performed on a Silicon Graphics 4D20 workstation.

The NMR input data is summarised in Table 3 and consisted of constraints derived from the NOE interactions, hydrogen bond distances and $^3J_{\text{NH-}\alpha\text{CH}}$ coupling constants. The NOE interactions were converted to an allowed proximity range. An NOE observed between two protons implies that the distance between the two atoms is less than approximately 5 Å. However a more restrictive upper limit can be specified to NOEs between backbone protons. Values have been estimated for the proton-proton distances in each of the common secondary structure elements *i.e.* α -helix, 3_{10} -helix, parallel and antiparallel β -sheet, and type I and type II turns.²⁴ The upper limit adopted in our calculations was the higher or highest value estimated for each intramolecular distance. The lower limit was set to the sum of

Table 3 Summary of constraints used in distance geometry calculations

	Distance constraint (Å)	δ -toxin ^a	δ -toxin ^b	Ac- δ -toxin ^b	Glu ⁸ - δ -toxin ^a	Glu ⁷ - δ -toxin ^a	Pro ¹⁴ - δ -toxin ^a	des-Lys ¹⁴ - δ -toxin ^b	Glu ⁸ , Pro ¹⁴ - δ -toxin ^b	
									Trp ¹⁵ (1)	Trp ¹⁵ (2)
d _{NN} (i, i + 1)	4.5	19	24	24	13	16	21	18	14	15
d _{NN} (i, i + 2)	4.3	1	1	10	0	0	1	0	2	2
d _{αN} (i, i + 1)	3.5	18	20	22	14	13	21	20	10	11
d _{βN} (i, i + 1)	4.7	19	25	21	12	19	14	23	11	13
d _{αN} (i, i + 3)	4.7	8	11	18	9	6	4	8	3	2
d _{αN} (i, i + 4)	4.2	5	10	9	5	5	1	2	3	2
d _{αB} (i, i + 3)	5.1	14	19	15	11	12	4	3	n.a.	n.a.
d _{αγ} (i, i + 3)	5.0	3	6	8	4	3	2	2	n.a.	n.a.
Proline interactions	5.0	—	—	—	—	—	4	—	4	6
Miscellaneous inter-residue interactions	—	20	110	59	21	12	11	20	33	33
Hydrogen bonds	2.9	13	19	21	13	12	5 ^c	14	n.a.	n.a.
φ-Torsion angles	—	7	10	11	14	0	16	15	6	6
Total ^d		107	145	159	95	86	93	105	53	57

^a Solvent = CD₃OH. ^b Solvent = CD₃OH-H₂O (2:1). ^c Only hydrogen bonds in α -helical segment included in structure determination. ^d Total not including miscellaneous inter-residue NOEs.



Fig. 11 (a) The seven α -carbon backbone structures of δ -toxin in methanol starting from the idealised α -helix conformation, superimposed to give the best-fit between residues 10 to 20. (b) As in (a) but eight structures starting from idealised β -sheet conformation.*



Fig. 12 (a) Seven α -carbon backbone structures of δ -toxin in methanol-water solution. Structures are superimposed to give the best-fit between residues 10 to 20. (b) Twelve α -carbon backbone structures of Ac- δ -toxin in methanol-water solution. Structures are superimposed to give the best-fit between residues 10 to 20.*

the appropriate van der Waals radii. The hydrogen bond distance corresponded to a constraint of 2.9 Å and these constraints were only added in when the basic α -helices were apparent from the NOE data. The torsion angles ϕ , calculated from the $^3J_{\text{NH-}\alpha\text{CH}}$ coupling constants, were confined to the range -30° to -180° .

Starting structures were either the idealised α -helix or β -sheet conformation of the peptide. DGEOM evolves structures by randomly varying the starting conformation and rejects those which violate either the distance or chiral constraints. The quality of each conformation was visually assessed and a structure was occasionally discarded if it appeared to be grossly atypical, but care was taken so as not to improperly bias the result in favour of the anticipated structure.

The results of the DGEOM and PIFF calculations for the

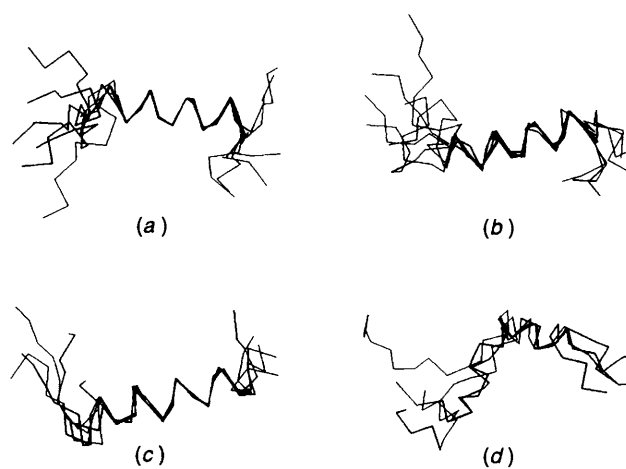


Fig. 13 α -Carbon backbone structures superimposed to give the best-fit in the α -helical regions. (a) Glu⁸- δ -toxin. (b) Glu⁷- δ -toxin. (c) des Lys¹⁴- δ -toxin. (d) Pro¹⁴- δ -toxin.*

CD₃OH structure of δ -toxin starting from both the idealised α -helix and β -sheet conformations are illustrated in Fig. 11. The structures are superimposed to give the best fit of the α -carbon chain between residues 10 and 20 and four turns of helix are clearly discernible. The similarity between Figs. 11(a) and 11(b) reassuringly reveal that the starting conformation is unimportant. The structures show good agreement in the central α -helical portion of the molecule which is an accurate reflection of the quality of the NMR data in this region. Both the *N*- and *C*-terminal ends were less well-defined by experimental constraints and exhibit a high degree of disorder in the calculated structures. Another feature revealed by the 3D structures, but not obvious in the black and white image of the α -carbon chain, is the amphiphilic nature of the α -helix and this confirms the predicted arrangement of the charged residues along one face of the helix.

Approximately five turns of the α -helix are observed in the calculated aqueous methanolic structures of δ -toxin and Ac- δ -toxin [Figs. 12(a) and 12(b), respectively]. Once again these calculated structures are reasonable interpretations of the NMR constraints with the *N*-terminus in particular being more consistent as a result of the long range NOEs in this region. In both of these structure determinations and also those of the

* General comment on Figs. 11–13: The peptide backbone runs from the *N*-terminus at the LHS of the diagram to the *C*-terminus at the RHS.

peptide analogues, only the β -sheet was used as the starting conformation.

Groups of conformers representing the result of the distance geometry and molecular mechanics calculations for Glu⁸-, Glu⁷- and the des-Lys¹⁴- δ -toxin are shown in Fig. 13. Four turns of the α -helix are readily defined for each molecule between approximately residues 8 and 22. The charged amino acids are amphiphically aligned within the helical segment of the Glu⁷ and Glu⁸ compounds whereas in des-Lys¹⁴- δ -toxin the aspartic acid at position 11 is offset by approximately 120° with respect to Asp¹⁸ and Lys²².

The calculated structures for Pro¹⁴- δ -toxin and Glu⁸, Pro¹⁴- δ -toxin were intuitively expected to be less precise. Both proline peptides adopt an L-shaped global conformation with a bend centred at residues 13/14. A couple of turns of helix between positions 15 and 22 are clearly visible in Pro¹⁴- δ -toxin [Fig. 13(d)] but in the Glu⁸, Pro¹⁴ analogue the lack of NMR constraints in this region translates into a much more variable structure although there is a distinct trend towards a helical segment (structures not shown). Two families of structures were obtained for Glu⁸, Pro¹⁴- δ -toxin in order to try and reflect the possible *cis-trans* isomerism about the Val¹³-Pro¹⁴ amide bond but the conformers were too variable to realistically detect any consistent differences.

No NMR spectroscopic data was available for Glu⁷, des-Lys¹⁴- δ -toxin due to the insolubility of this peptide in methanol and methanol-water mixtures. However, experience with compounds 4 and 6 suggests that, under the appropriate conditions, the structure of Glu⁷, des-Lys¹⁴- δ -toxin is probably similar to that of des-Lys¹⁴- δ -toxin.

Thus, a combination of 2D NMR experiments and molecular modelling techniques clearly demonstrates that δ -toxin and a number of closely related analogues assume well-ordered three-dimensional structures in methanol or methanol-water solutions. The extent of helical character in δ -toxin is apparently partially influenced by the composition of the solvent and partially by the polarity of the *N*-terminal amino acid. In this series of analogue compounds the helical segment survives minor modification to the peptide sequence towards the *N*-terminus but is radically curtailed by incorporation of a proline in the centre of the molecule. Multiple sequence changes cause insolubility and handling problems in the resulting peptides.

The structures generated by the distance geometry algorithm were based on backbone NMR spectroscopic data and only a vague indication of the spatial arrangement of the side chains was perceived. More sophisticated calculations incorporating side-chain to side-chain interactions are planned. Viewed from the standpoint of the criteria of Eisenberg and co-workers²⁵ the proposed monomeric helical structures for these small peptides are unlikely and it is more probable that they exist as transiently formed higher oligomers. Structures for δ -toxin and Ac- δ -toxin have been deposited in Brookhaven Protein Data Bank²⁶ (reference codes 2DTB and 1DTC respectively). Data for the other structures are in the process of being deposited.

Ion channel studies on this series of compounds are in progress. Preliminary results with δ -toxin and Ac- δ -toxin indicate that the synthetic compounds are behaving as expected and voltage-dependent ion channels are being formed. Full details of these and other experiments will be reported in due course.

Experimental

Materials.—Fmoc amino acids and resins were purchased from Novabiochem. Other reagents for peptide synthesis were dimethylformamide (DMF) (peptide synthesis grade, Rathburn), dioxane (Rathburn), piperidine (peptide synthesis grade, Rathburn), 1-hydroxybenzotriazole hydrate (HOBt) (Fluka),

trifluoroacetic acid (TFA) (Applied Biosystems), MeCN (HPLC grade, Rathburn) and water (purified by MilliQ water purification system). All other reagents were of analytical grade and purchased from general laboratory suppliers. HPLC was carried out on an Applied Biosystems 151A Separation System. Peptide samples were analysed on Aquapore RP-300 C₈ or C₁₈ analytical columns (4.6 × 100 mm) and purified on preparative columns, either Aquapore RP-300 C₈ or C₁₈ (10 × 100 mm) or Vydac C₁₈ (20 × 220 mm). Samples for preparative HPLC were filtered (0.45 μ m membranes) prior to purification. Peptides were eluted with linear gradients composed of 0.1% aqueous TFA and 0.1% TFA in MeCN. Elution was at a flow rate of 1 cm³ min⁻¹ and 5 cm³ min⁻¹ for the analytical and preparative Aquapore columns respectively and 10 cm³ min⁻¹ for the Vydac column. Peaks were detected at 230 nm. Samples for amino acid analysis were prepared by sealed tube hydrolysis with constant boiling HCl containing a small amount of phenol at 110 °C for 24 h and analysed on an LKB 4151 instrument. Fast atom bombardment mass spectra were recorded on a Kratos MS 50TC spectrometer.

Peptide Synthesis and Purification.—Peptides were synthesised either on a semi-automatic continuous flow instrument (Cambridge Research Biochemicals Pepsynthesiser) using Sheppard's Fmoc-polyamide method,²⁷ or on a fully-automated batch instrument (Applied Biosystems 430A) utilising a polystyrene resin as the solid support and Fmoc as the N α -protecting group. Side chain functionalities were protected as follows: Asp(OBu^t), Ser(Bu^t), Thr(Bu^t) and Lys(Boc). In the semi-automated syntheses the resin (Macrosorb SPR, 1.5 g 0.1 mmol dm⁻³ g⁻¹) was functionalised with the 3-methoxy-4-hydroxymethylphenoxyacetic acid linker and the acylating reactions were carried out in a single coupling step in DMF with a four-fold excess of either the symmetrical anhydride or pentafluorophenyl ester (apart from Asn and Gln which were coupled as the *p*-nitrophenyl esters). Coupling reactions were monitored by the ninhydrin²⁸ and trinitrobenzene sulfonic acid²⁹ colour tests and all were completed within 2 h apart from Gln which required a repeat coupling. The progress of synthesis was checked several times by total acid hydrolysis and subsequent amino acid hydrolysis of small aliquots of peptide resin. In each case the progress was satisfactory. In the fully-automated approach the Wang resin³⁰ (1 g, 0.8 mmol dm⁻³ g⁻¹) and a double coupling procedure was used. A two-fold excess of the symmetrical anhydride was followed by a two-fold excess of the HOBt ester apart for Gly which was single coupled with a four-fold excess of the symmetrical anhydride and Asn, Gln which were activated by the HOBt method in a double coupling. Coupling reactions were carried out in 1:1 DMF-dioxane mixtures for 30 min each and after each coupling phase any unchanged amino groups were capped using Ac₂O. The progress of the synthesis was followed by a method developed by Ramage and co-workers in which the deprotection of the N α -Fmoc group was continuously monitored by UV spectroscopy at 302 nm and the areas under the peaks were calculated to give a quantitative assessment of the combined coupling and deprotection stages. Acetylated derivatives were prepared by treating the completed resin-bound peptide with an excess of Ac₂O. Peptides were cleaved from the resins by treatment with TFA-anisole-ethane-1,2-dithiol (9:0.5:0.5) for 1–3 h at room temp. under nitrogen. The resin was filtered, the filtrate was concentrated under reduced pressure and the peptide was precipitated by the addition of ether. Crude peptides were shown by analytical HPLC to contain one major peak and were generally >60–70% pure at this stage. All the peptides were purified in a two-step procedure. The crude peptide was first applied to a column of Sephadex 25 (fine, 2.5 × 85 cm) which was eluted with 0.2 mol dm⁻³ AcOH (apart from compounds 7

and **7a** which were eluted with 20% AcOH). Fractions corresponding to the main peak were pooled and lyophilised. The peptides were further purified by reversed-phase HPLC. The purest fractions were then pooled and lyophilised. The purified peptides were >95% pure on analytical HPLC and were subjected to amino acid analysis and fast-atom bombardment mass spectrometry to confirm their composition. Amino acid ratios in acid hydrolysates were referenced to phenylalanine. Isoleucine values are low due to incomplete hydrolysis of the sterically hindered Ile-Ile moieties. Tryptophan was not determined and figures in parentheses stand for theoretical values. Calculated molecular masses assume one C-13 atom.

NMR Data Acquisition and Analyses.—All NMR data sets were acquired at 600 MHz (¹H) on a Varian VXR 600S spectrometer equipped with a Sun 4/110 host computer running the VNMR system software version 3.1. Data were acquired using either a dedicated proton probehead or an inverse probehead. For most purposes probe temperature was maintained at 303K ± 0.1 K. Sets of data consisting of DQF COSY, TOCSY, NOESY and a single pulse acquisition were acquired sequentially without removal of the sample from the magnet. In all cases, the carrier frequency was placed at the CD₃OH resonance at the centre of the spectrum. All two-dimensional acquisitions were carried out with a non-spinning sample. In all cases of samples dissolved in CD₃OH or CD₃OH–H₂O mixtures, water-suppression was achieved by means of low power transmitter presaturation during the recycle delay of each type of experiment without any detrimental effect to the quality of the data. Conditions are described for all two-dimensional experiments carried out on Ac-δ-toxin, which are typical for all the δ-toxin analogues.

Pure absorption two-dimensional DQF COSY, TOCSY and NOESY data were collected with quadrature detection into 2048 complex data points for 2 × 200t₁ increments in the hypercomplex phase sensitive mode.³¹ 32 transients were acquired for each t₁ increment with a recycle delay of 2.5 s. Data were acquired over a 7 kHz spectral width to give a final f₂ digital resolution of 3.42 Hz per point. A standard mixing time of 80 ms was used in the TOCSY experiment. A mixing time of 300 ms was randomly varied by 3% over the entire NOESY experiment.

One-dimensional spectra of samples dissolved in CD₃OH or CD₃OH–H₂O mixtures were acquired spinning using a transmitter solvent suppression technique; 128 transients were acquired into 42 K data points over a 7 kHz spectral width with a recycle delay of 2.5 s to give a final digital resolution of 0.1 Hz per point.

One-dimensional 'exchange' spectra were acquired on samples dissolved in perdeuterated solvent. Typically an array of 16 spectra were acquired without removal of the sample from the magnet. The fully protonated sample was dissolved in CD₃OD or the CD₃OD–D₂O mixture just prior to insertion into the probe. The first spectrum was acquired as soon as possible after insertion and subsequent spectra were acquired at increasing time intervals; 64 transients were acquired into 42 K data points over a 7 kHz spectral width with a recycle delay of 2.5 s to give a final digital resolution of 0.16 Hz per point.

All data were transferred to a remote Sun 4/330 data station for processing using VNMR 3.1 software. 2D data sets were transformed by zero filling in f₁ to 1024 K data points before apodisation in both dimensions using π/4 shifted squared sinebell window function prior to Fourier transformation. One-dimensional data sets were transformed after zero-filling into 65 K data points.

In the following assignments when only one chemical shift is given for a methylene group it could not be established whether

the resonances of the two protons were degenerate or whether the second resonance could not be observed. All *J* values are given in Hz.

δ-Toxin 1. Amino acid ratios: Met(1) 0.79, Ala(1) 0.93, Glu(1) 1.00, Asp(4) 4.07, Ile(5) 4.11, Ser(1) 0.84, Thr(3) 2.77, Gly(1) 0.98, Leu(1) 0.96, Val(2) 1.97, Lys(4) 3.81, Phe(1) 1.00 (Found: MH⁺ 2978.64692. C₁₃₆H₂₂₆N₃₃O₃₉S⁺ requires *M*, 2978.64687) δ_H(c 6.0 mmol dm⁻³ in CD₃OH; 600 MHz) Met¹: αCH(4.00), βCH₂(2.21, 2.11), γCH₂(2.61), εCH₃(2.13); Ala²: NH(8.86), αCH(4.29), βCH₃(1.42); Gln³: NH(8.68), αCH(4.18), βCH₂(2.05, 1.98), γCH₂(2.34), δNH₂(7.50, 6.73); Asp⁴: NH(8.31), αCH(4.62), βCH₂(2.89); Ile⁵: NH(8.12), αCH(3.98), βCH(1.96), γCH₂(1.60, 1.28), γCH₃(0.96^a), δCH₃-(0.91^a); Ile⁶: NH(7.76), αCH(3.78), βCH(1.99), γCH₂(1.59, 1.23), γCH₃(0.92^b), δCH₃(0.86^b); Ser⁷: NH(8.06), αCH(4.22), βCH₂(3.94, 3.85); Thr⁸: NH(7.85), αCH(3.98), βCH(4.29), γCH₃(1.20); Ile⁹: NH(8.19), αCH(3.74), βCH(1.96), γCH₂(1.75, 1.20), γCH₃(0.92^c), δCH₃(0.82^c); Gly¹⁰: NH(8.46), αCH₂(3.85, 3.72); Asp¹¹: NH(8.28), αCH(4.42), βCH₂(3.11, 2.70); Leu¹²: NH(8.06), αCH(4.22), βCH₂(1.86), γCH(1.86), δCH₃(0.96, 0.90); Val¹³: NH(8.46), αCH(3.58), βCH(2.25), γCH₃(1.10, 0.95); Lys¹⁴: NH(8.11), αCH(3.87), βCH₂(1.96), γCH₂(1.42), δCH₂(1.65), εCH₂(2.93); Trp¹⁵: NH(8.32), αCH(4.31), βCH₂-(3.59, 3.38), 2H(7.09), 4H(7.50), 5H(6.95), 6H(7.06), 7H(7.32), NH(10.13); Ile¹⁶: NH(8.63), αCH(3.48), βCH(2.13), γCH₂-(1.17), γ, δCH₃(0.90); Ile¹⁷: NH(8.49), αCH(3.54), βCH(1.94), γCH₂(1.79, 1.16), γCH₃(0.90), δCH₃(0.80); Asp¹⁸: NH(8.74), αCH(4.36), βCH₂(2.94, 2.62); Thr¹⁹: NH(8.03), αCH(3.69), βCH(4.03), γCH₃(0.96); Val²⁰: NH(8.41), αCH(3.66), βCH-(2.17), γCH₃(1.02, 0.93); Asn²¹: NH(8.32), αCH(4.50), βCH₂-(2.88, 2.69), γNH₂(7.63, 6.84); Lys²²: NH(7.92), αCH(3.94), βCH₂(1.78, 1.65), γCH₂(1.40, 1.19), δCH₂(1.51), εCH₂(2.76); Phe²³: NH(7.94), αCH(4.50), βCH₂(3.25, 3.04), 2,6H(7.32^d), 3,5H(7.22^d), 4H(7.19^d); Thr²⁴: NH(7.74), αCH(4.26), βCH-(4.26), γCH₃(1.26); Lys²⁵: NH(8.01), αCH(4.22), βCH₂(1.86), γCH₂(1.47), δCH₂(1.64), εCH₂(2.92); Lys²⁶: NH(8.03), αCH-(4.36), βCH₂(1.90, 1.75), γCH₂(1.45), δCH₂(1.63), εCH₂(2.90), (^{a,b,c,d}these have not been unambiguously assigned and may be reversed); ³J_{NH CH}: Ala² (ca. 4.0), Gln³(5.1), Thr⁸(2.9), Ile⁹(3.1), Ile¹⁶(3.6), Asp¹⁸(1.9), Val²⁰(3.1); slow NH exchange, present after 15 h: Val¹³, Lys¹⁴, Trp¹⁵, Ile¹⁶, Ile¹⁷, Asp¹⁸, Thr¹⁹, Val²⁰, Asn²¹, exchange < 15 h: Asp¹¹, Leu¹², Lys²² and Phe²³. δ_H[c. 4.8 mmol dm⁻³ in CD₃OH–H₂O (2:1); 600 MHz] Met¹: αCH(4.15), βCH₂(2.24, 2.20), γCH₂(2.67), εCH₃(2.13); Ala²: NH(8.87), αCH(4.40), βCH₃(1.49); Gln³: NH(8.63), αCH(4.29), βCH₂(2.12, 2.05), γCH₂(2.42), δNH₂(7.59, 6.86); Asp⁴: NH(8.53), αCH(4.72), βCH₂(2.96); Ile⁵: NH(8.21), αCH(4.10), βCH(2.01), γCH₂(1.60, 1.33), γCH₃(1.00^a), δCH₃(0.96^a); Ile⁶: NH(7.93), αCH(3.92), βCH(2.03), γCH₂(1.63, 1.30), γCH₃-(0.99^b), δCH₃(0.92^b); Ser⁷: NH(8.18), αCH(4.37), βCH₂(4.00, 3.93); Thr⁸: NH(7.97), αCH(4.16), βCH(4.40), γCH₃(1.29); Ile⁹: NH(8.15), αCH(3.87), βCH(2.02), γCH₂(1.73, 1.29), γCH₃(0.99^c), δCH₃(0.91^c); Gly¹⁰: NH(8.47), αCH₂(3.97, 3.80); Asp¹¹: NH(8.26), αCH(4.52), βCH₂(3.17, 2.85); Leu¹²: NH(8.10), αCH(4.32), βCH₂(1.91), γCH(1.86), δCH₃(1.03, 0.96); Val¹³: NH(8.51), αCH(3.66), βCH(2.29), γCH₃(1.16, 1.03); Lys¹⁴: NH(8.05), αCH(3.95), βCH₂(2.03), γCH₂(1.50), δCH₂(1.77, 1.67), εCH₂(3.04); Trp¹⁵: NH(8.25), αCH(4.37), βCH₂(3.69, 3.43), 2H(7.20), 4H(7.60), 5H(7.01), 6H(7.16), 7H(7.42), NH(10.18); Ile¹⁶: NH(8.72), αCH(3.46), βCH(2.19), γCH₂(n.a.), γ,δCH₃(0.94); Ile¹⁷: NH(8.50), αCH(3.61), βCH-(1.99), γCH₂(1.81, 1.21), γCH₃(0.97), δCH₃(0.87); Asp¹⁸: NH(8.70), αCH(4.44), βCH₂(3.05, 2.75); Thr¹⁹: NH(8.06), αCH(3.79), βCH(3.98), γCH₃(0.98); Val²⁰: NH(8.40), αCH-(3.74), βCH(2.21), γCH₃(1.06, 0.99); Asn²¹: NH(8.28), αCH-(4.58), βCH₂(2.90, 2.78), γNH₂(7.68, 6.92); Lys²²: NH(7.86), αCH(4.06), βCH₂(1.81, 1.71), γCH₂(1.37, 1.20), δCH₂(1.59), εCH₂(2.87); Phe²³: NH(7.96), αCH(4.63), βCH₂(3.35, 3.06),

2,6H(7.40^d), 3,5H(7.32^d), 4H(7.28^d); Thr²⁴: NH(7.79), α CH-(4.36), β CH(4.30), γ CH₃(1.32); Lys²⁵: NH(8.11), α CH-(4.34), β CH₂(1.93, 1.89), γ CH₂(1.54), δ CH₂(1.73), ϵ CH₂(3.02); Lys²⁶: NH(8.25), α CH(4.42), β CH₂(1.97, 1.82), γ CH₂(1.52), δ CH₂(1.72), ϵ CH₂(3.02), (^{a,b,c,d}these have not been unambiguously assigned and may be reversed); ³J_{NH- α CH: Ala²(5.1), Gln³(5.4), Asp⁴(5.6), Ile⁵(ca. 6), Ser⁷(ca. 4), Ile⁹(ca. 6), Val²⁰(ca. 5), Lys²²(ca. 4), Thr²⁴(7.1), Lys²⁵(7.1); slow NH exchange, present after 17 h: Val¹³, Lys¹⁴, Trp¹⁵, Ile¹⁶, Ile¹⁷, Asp¹⁸, Thr¹⁹, Val²⁰, exchange < 17 h: Ile⁶, Thr⁸, Ile⁹, Gly¹⁰, Asp¹¹, Leu¹², Asn²¹, Lys²², Phe²³, Thr²⁴ and Lys²⁵.}

Ac- δ -toxin 1a. Amino acid ratios: Met(1) 0.83, Ala(1) 0.93, Glu(1) 1.04, Asp(4) 3.80, Ile(5) 4.02, Ser(1) 0.81, Thr(3) 2.65, Gly(1) 0.97, Leu(1) 1.02, Val(2) 1.94, Lys(4) 3.85, Phe(1) 1.00 (Found: MH⁺ 3020.65749. C₁₃₈H₂₂₈N₃₃O₄₀S⁺ requires *M*, 3020.65744) $\delta_{\text{H}}[c$ 1.7 mmol dm⁻³ in CD₃OH-H₂O (2:1); 600 MHz] Met¹: NH(8.38), α CH(4.39), β CH₂(2.04, 2.02), γ CH₂(2.60, 2.56), ϵ CH₃(2.07^a), CH₃CO(2.04^a); Ala²: NH(8.59), α CH(4.14), β CH₃(1.44); Gln³: NH(8.35), α CH(4.10), β CH₂(2.09), γ CH₂(2.42, 2.36), δ NH₂(7.57, 6.82); Asp⁴: NH(8.27), α CH(4.58), β CH₂(3.02, 2.98); Ile⁵: NH(8.19), α CH(3.88), β CH(2.00), γ CH₂(1.68, 1.21), γ CH₃(0.94), δ CH₃(0.88); Ile⁶: NH(8.05), α CH(3.80), β CH(1.96), γ CH₂(1.65, 1.24), γ CH₃(0.95), δ CH₃(0.86); Ser⁷: NH(8.26), α CH(4.29), β CH₂(4.02, 3.94); Thr⁸: NH(7.98), α CH(4.07), β CH(4.38), γ CH₃(1.24); Ile⁹: NH(8.32), α CH(3.80), β CH(1.99), γ CH₂(1.74, 1.24), γ CH₃(0.94), δ CH₃(0.86); Gly¹⁰: NH(8.45), α CH₂(3.96, 3.80); Asp¹¹: NH(8.24), α CH(4.49), β CH₂(3.16, 2.82); Leu¹²: NH(8.09), α CH(4.28), β CH₂(1.89), γ CH(1.83), δ CH₃(0.97, 0.91); Val¹³: NH(8.49), α CH(3.63), β CH(2.25), γ CH₃(1.12, 0.98); Lys¹⁴: NH(8.02), α CH(3.92), β CH₂(1.99), γ CH₂(1.44), δ CH₂(1.71, 1.63), ϵ CH₂(2.98); Trp¹⁵: NH(8.20), α CH(4.33), β CH₂(3.65, 3.40), 2H(7.14), 4H(7.54), 5H(6.96), 6H(7.12), 7H(7.37), NH(10.13); Ile¹⁶: NH(8.68), α CH(3.44), β CH(2.14), γ CH₂(1.18), γ CH₃(0.92^b), δ CH₃(0.88^b); Ile¹⁷: NH(8.45), α CH(3.58), β CH(1.94), γ CH₂(1.78, 1.19), γ CH₃(0.92), δ CH₃(0.82); Asp¹⁸: NH(8.65), α CH(4.41), β CH₂(2.97, 2.72); Thr¹⁹: NH(8.01), α CH(3.77), β CH(3.96), γ CH₃(0.93); Val²⁰: NH(8.35), α CH(3.71), β CH(2.16), γ CH₃(1.01, 0.94); Asn²¹: NH(8.22), α CH(4.56), β CH₂(2.88, 2.77), γ NH₂(7.64, 6.88); Lys²²: NH(7.81), α CH(4.03), β CH₂(1.75, 1.66), γ CH₂(1.31, 1.14), δ CH₂(1.53), ϵ CH₂(2.81); Phe²³: NH(7.91), α CH(4.60), β CH₂(3.32, 3.03), 2, 6H(7.34^c), 3, 5 H(7.27), 4 H(7.22^c); Thr²⁴: NH(7.73), α CH(4.32), β CH(4.27), γ CH₃(1.27); Lys²⁵: NH(8.09), α CH(4.32), β CH₂(1.88, 1.83), γ CH₂(1.48), δ CH₂(1.68), ϵ CH₂(2.96); Lys²⁶: NH(8.20), α CH-(4.38), β CH₂(1.91, 1.76), γ CH₂(1.46), δ CH₂(1.67), ϵ CH₂(2.95), (^{a,b,c,d}these have not been unambiguously assigned and may be reversed); ³J_{NH- α CH: Met¹(5.3), Ala²(4.0), Ile⁶(ca. 5.3), Thr⁸(4.6), Ile⁹(ca. 3.5), Val¹³(< 3.0), Ile¹⁶(< 3.0), Asp¹⁸(< 3.0), Lys²²(4.2), Phe²³(7.2), Thr²⁴(7.5); slow NH exchange, present after 15 h: Gly¹⁰, Asp¹¹, Leu¹², Val¹³, Lys¹⁴, Trp¹⁵, Ile¹⁶, Ile¹⁷, Asp¹⁸, Thr¹⁹, Val²⁰, Asn²¹, exchange < 15 h: Ala², Asp⁴, Ile⁵, Ile⁶, Ser⁷, Thr⁸, Ile⁹, Lys²², Phe²³ and Thr²⁴.}

Glu⁸- δ -toxin 2. Amino acid ratios: Met(1) 0.94, Ala(1) 0.92, Glu(2) 2.14, Asp(4) 3.99, Ile(5) 4.33, Ser(1) 0.78, Thr(2) 1.75, Gly(1) 0.96, Leu(1) 0.99, Val(2) 1.99, Lys(4) 3.77, Phe(1) 1.00 (Found: MH⁺ 3006.64186. C₁₃₇H₂₂₆N₃₃O₄₀S⁺ requires *M*, 3006.64179) $\delta_{\text{H}}[c$ 5.9 mmol dm⁻³ in CD₃OH; 600 MHz] Met¹: α CH(4.09), β CH₂(2.24, 1.99), γ CH₂(2.68), ϵ CH₃(2.18); Ala²: NH(8.83), α CH(4.40), β CH₃(1.47); Gln³: NH(8.52), α CH(4.36), β CH₂(2.02), γ CH₂(2.41, 2.14), δ NH₂(7.57, 6.84); Asp⁴: NH(8.43), α CH(4.76), β CH₂(2.94, 2.88); Ile⁵: NH(ca. 8.00), α CH(3.50), β CH(1.41), γ CH₂(1.33), γ , δ CH₃(0.93); Ile⁶: NH(8.00), α CH(4.26), β CH(1.98), γ CH₂(1.56, 1.26), γ , δ CH₃(0.93); Ser⁷: NH(8.07), α CH(4.50), β CH₂(3.89); Glu⁸: NH(8.12), α CH-(4.48), β CH(2.10), γ CH₂(2.56, 2.35); Ile⁹: NH(8.47), α CH(4.09), β CH(1.95), γ CH₂(1.60, 1.38), γ CH₃(1.04), δ CH₃(0.99); Gly¹⁰: NH(8.82), α CH₂(3.89); Asp¹¹: NH(7.96), α CH(3.59), β CH₂-

(3.03, 2.86); Leu¹²: NH(8.02), α CH(4.31), β CH₂(1.84), γ CH(1.93), δ CH₃(1.07, 0.99); Val¹³: NH(8.23), α CH-(3.70), β CH(2.24), γ CH₃(1.16, 1.04); Lys¹⁴: NH(7.79), α CH-(3.98), β CH₂(2.00), γ CH₂(1.48), δ CH₂(1.75, 1.65), ϵ CH₂(3.02); Trp¹⁵: NH(8.18), α CH(4.39), β CH₂(3.63, 3.45), 2H(7.17), 4H(7.58), 5H(7.03), 6H(7.16), 7H(7.42), NH(10.22); Ile¹⁶: NH(8.60), α CH(3.57), β CH(2.16), γ CH₂(1.25), γ , δ CH₃(0.97); Ile¹⁷: NH(8.46), α CH(3.64), β CH(1.99), γ CH₂(1.84, 1.25), γ CH₃(0.98), δ CH₃(0.88); Asp¹⁸: NH(8.68), α CH(4.46), β CH₂(3.05, 2.79); Thr¹⁹: NH(8.06), α CH(3.83), β CH(4.09), γ CH₃(1.04); Val²⁰: NH(8.42), α CH(3.77), β CH(2.23), γ CH₃(1.09, 1.01); Asn²¹: NH(8.29), α CH(4.60), β CH₂(2.92, 2.80), γ NH₂(7.65, 6.92); Lys²²: NH(7.90), α CH(4.06), β CH₂(1.83, 1.72), γ CH₂(1.40, 1.24), δ CH₂(1.59), ϵ CH₂(2.87); Phe²³: NH(7.99), α CH(4.62), β CH₂(3.36, 3.09), 2, 6H(7.42^a), 3, 5H(7.32), 4H-(7.26^a); Thr²⁴: NH(7.79), α CH(4.34), β CH(4.34), γ CH₃(1.34); Lys²⁵: NH(8.11), α CH(4.34), β CH₂(1.92), γ CH₂(1.55), δ CH₂(1.73), ϵ CH₂(3.01); Lys²⁶: NH(8.22), α CH(4.46), β CH₂(1.98, 1.82), γ CH₂(1.52), δ CH₂(1.72), ϵ CH₂(3.00), (^athese have not been unambiguously assigned and may be reversed); ³J_{NH- α CH: Gln³(6.7), Ser⁷(7.4), Glu⁸(7.5), Asp¹¹(5.4), Leu¹²(4.5), Lys¹⁴(6.7), Trp¹⁵(3.4), Ile¹⁶(3.8), Asp¹⁸(3.2), Thr¹⁹(3.4), Asn²¹(4.5), Lys²²(5.0), Lys²⁵(5.7), Lys²⁶(8.2); slow NH exchange, present after 12 h: Val¹³, Lys¹⁴, Trp¹⁵, Ile¹⁶, Ile¹⁷, Asp¹⁸, Thr¹⁹, Val²⁰, exchange < 12 h: Asp¹¹, Leu¹², Asn²¹, Lys²² and Phe²³.}

Ac-Glu⁸- δ -toxin 2a. Amino acid ratios: Met(1) 0.84, Ala(1) 0.77, Glu(2) 1.99, Asp(4) 4.10, Ile(5) 3.78, Ser(1) 0.85, Thr(2) 1.88, Gly(1) 0.73, Leu(1) 0.93, Val(2) 1.98, Lys(4) 3.85, Phe(1) 1.00 (Found: MH⁺ 3048.65242. C₁₃₉H₂₂₈N₃₃O₄₁S⁺ requires *M*, 3048.65235).

Glu⁷- δ -toxin 3. Amino acid ratios: Met(1) 0.92, Ala(1) 1.02, Glu(2) 2.37, Asp(4) 3.92, Ile(5) 3.47, Thr(3) 2.81, Gly(1) 1.15, Leu(1) 0.99, Val(2) 1.94, Lys(4) 3.77, Phe(1) 1.00 (Found: MH⁺ 3020.65749. C₁₃₈H₂₂₈N₃₃O₄₀S⁺ requires *M*, 3020.65744) $\delta_{\text{H}}[c$ 7.0 mmol dm⁻³ in CD₃OH; 600 MHz] Met¹: α CH(4.02), β CH₂(2.19, 2.12), γ CH₂(2.60), ϵ CH₃(2.13); Ala²: NH(8.75), α CH-(4.37), β CH₃(1.41); Gln³: NH(8.25), α CH(4.39), β CH₂(2.00), γ CH₂(2.45, 2.17), δ NH₂(7.51, 6.84); Asp⁴: NH(8.06), α CH-(4.40), β CH₂(3.13, 2.74); Ile⁵: NH(7.93), α CH(4.22), β CH(1.82), γ CH₂(1.16), γ , δ CH₃(0.87); Ile⁶: NH(7.94), α CH(4.16), β CH-(1.85), γ CH₂(1.50, 1.15), γ CH₃(0.90^a), δ CH₃(0.82^a); Glu⁷: NH(8.45), α CH(4.32), β CH₂(1.96), γ CH₂(2.34, 2.08); Thr⁸: NH(7.80), α CH(4.43^b), β CH(4.37^b), γ CH₃(1.24); Ile⁹: NH(8.55), α CH(3.95), β CH(1.92), γ CH₂(1.64, 1.33), γ CH₃(0.98^c), δ CH₃(0.96^c); Gly¹⁰: NH(8.22), α CH₂(3.90, 3.74); Asp¹¹: NH(8.28), α CH(4.72), β CH₂(2.85, 2.75); Leu¹²: NH(7.87), α CH(4.24), β CH₂(1.84), γ CH(1.79), δ CH₃(0.97, 0.91); Val¹³: NH(8.33), α CH(3.61), β CH(2.24), γ CH₃(1.10, 0.97); Lys¹⁴: NH(8.05), α CH(3.90), β CH₂(1.98), γ CH₂(1.43), δ CH₂(1.68), ϵ CH₂(2.95); Trp¹⁵: NH(8.32), α CH(4.32), β CH₂(3.58, 3.40), 2H(7.09), 4H(7.53), 5H(6.98), 6H(7.09), 7H(7.35), NH(10.20); Ile¹⁶: NH(8.65), α CH(3.53), β CH(2.14), γ CH₂(1.20), γ , δ CH₃(0.92); Ile¹⁷: NH(8.50), α CH(3.58), β CH(1.95), γ CH₂(1.81, 1.17), γ CH₃(0.92), δ CH₃(0.82); Asp¹⁸: NH(8.73), α CH(4.40), β CH₂(3.01, 2.70); Thr¹⁹: NH(8.07), α CH(3.72), β CH(4.06), γ CH₃(0.99); Val²⁰: NH(8.43), α CH(3.69), β CH(2.19), γ CH₃(1.04, 0.96); Asn²¹: NH(8.31), α CH(4.53), β CH₂(2.89, 2.73), γ NH₂(7.59, 6.89); Lys²²: NH(7.93), α CH(3.98), β CH₂(1.82, 1.68), γ CH₂(1.43, 1.22), δ CH₂(1.54), ϵ CH₂(2.80); Phe²³: NH(7.97), α CH(4.52), β CH₂(3.27, 3.07), 2, 6H(7.37^d), 3, 5H(7.25), 4H(7.22^d); Thr²⁴: NH(7.79), α CH(4.29), β CH(4.29), γ CH₃(1.30); Lys²⁵: NH(8.04), α CH(4.24), β CH₂(1.89), γ CH₂(1.48), δ CH₂(1.67), ϵ CH₂(2.94); Lys²⁶: NH(8.09), α CH(4.41), β CH₂(1.90, 1.78), γ CH₂(1.45), δ CH₂(1.64), ϵ CH₂(2.94), (^{a,b,c,d}these have not been unambiguously assigned and may be reversed); slow NH exchange, present after 12 h: Trp¹⁵, Ile¹⁶, Ile¹⁷, Asp¹⁸, Thr¹⁹, Val²⁰, Asn²¹, exchange < 12 h: Leu¹², Val¹³, Lys¹⁴, Lys²² and Phe²³.

Ac-Glu⁷-δ-toxin 3a. Amino acid ratios: Met(1) 0.79, Ala(1) 0.99, Glu(2) 2.18, Asp(4) 4.07, Ile(5) 4.31, Thr(3) 2.78, Gly(1) 1.03, Leu(1) 1.06, Val(2) 2.04, Lys(4) 4.07, Phe(1) 1.00 (Found: MH⁺ 3062.66787. C₁₄₀H₂₃₀N₃₃O₄₁S⁺ requires *M*, 3062.66800).

Pro¹⁴-δ-toxin 4. Amino acid ratios: Met(1) 0.91, Ala(1) 0.99, Glu(1) 1.00, Asp(4) 4.01, Ile(5) 3.86, Ser(1) 0.87, Thr(3) 2.83, Gly(1) 1.00, Leu(1) 1.02, Val(2) 1.97, Pro(1) 1.00, Lys(3) 2.97, Phe(1) 1.00 (Found: MH⁺ 2947.60460. C₁₃₅H₂₂₁N₃₂O₃₉S⁺ requires *M*, 2947.60468) δ_H[c 4.3 mmol dm⁻³ in CD₃OH; 600 MHz] Met¹: αCH(4.07), βCH₂(2.23, 2.17), γCH₂(2.65), εCH₃(2.13); Ala²: NH(8.78), αCH(4.39), βCH₃(1.46); Gln³: NH(8.50), αCH(4.31), βCH₂(2.11, 2.01), γCH₂(2.38), δNH₂(7.50, 6.78); Asp⁴: NH(8.41), αCH(4.74), βCH₂(2.95, 2.89); Ile⁵: NH(8.07), αCH(4.15), βCH(1.97), γCH₂(1.56, 1.28), γCH₃(0.96^a), δC-H₃(0.92^a); Ile⁶: NH(*ca.* 7.90), αCH(3.47), βCH(1.97), γCH₂(1.38, 1.31), γCH₃(0.96^b), δCH₃(0.90^b); Ser⁷: NH(7.99), αCH(4.42), βCH₂(3.87, 3.96); Thr⁸: NH(7.87), αCH(4.27), βCH(4.36), γCH₃(1.25); Ile⁹: NH(7.97), αCH(4.03), βCH(1.98), γCH₂(1.64, 1.29), γCH₃(0.96^c), δCH₃(0.90^c); Gly¹⁰: NH(8.30), αCH₂(3.90); Asp¹¹: NH(8.02), αCH(4.75), βCH₂(2.95); Leu¹²: NH(8.06), αCH(4.50), βCH₂(1.89), γCH(1.78), δCH₃(0.98, 0.89); Val¹³: NH(7.98), αCH(3.91), βCH(2.35), γCH₃(1.16, 0.97); Pro¹⁴: αCH(4.20), βCH₂(2.28, 1.76), γCH₂(2.14, 1.95), δCH₂(3.72); Trp¹⁵: NH(7.38), αCH(4.40), βCH₂(3.49, 3.40), 2-H(7.23), 4H(7.54), 5H(7.01), 6H(7.11), 7H(7.37), NH(10.25); Ile¹⁶: NH(8.29), αCH(3.66), βCH(2.11), γCH₂(1.88, 1.18), γ,δCH₃(0.94); Ile¹⁷: NH(8.18), αCH(3.66), βCH(1.94), γCH₂(1.69, 1.23), γCH₃(0.95), δCH₃(0.84); Asp¹⁸: NH(8.37), αCH(4.46), βCH₂(3.01, 2.82); Thr¹⁹: NH(7.92), αCH(3.89), βCH(4.19), γCH₃(1.12); Val²⁰: NH(8.27), αCH(3.78), βCH(2.20), γCH₃(1.07, 0.99); Asn²¹: NH(8.22), αCH(4.60), βCH₂(2.89, 2.79), γNH₂(7.57, 6.85); Lys²²: NH(7.90), αCH(4.04), βCH₂(1.80, 1.70), γCH₂(1.39, 1.25), δCH₂(1.59), εCH₂(2.86); Phe²³: NH(7.95), αCH(4.62), βCH₂(3.33, 3.08), 2, 6H(7.34^d), 3, 5H(7.27), 4H(7.22^d); Thr²⁴: NH(7.73), αCH(4.34), βCH(4.31), γCH₃(1.31); Lys²⁵: NH(8.04), αCH(4.32), βCH₂(1.91), γCH₂(1.52), δCH₂(1.71), εCH₂(2.99); Lys²⁶: NH(8.15), αCH(4.44), βCH₂(1.96, 1.80), γCH₂(1.50), δCH₂(1.69), εCH₂(2.99), (^{a,b,c,d}these have not been unambiguously assigned and may be reversed); ³J_{NH-αCH}: Ala²(5.6), Gln³(6.4), Asp⁴(7.1), Ile⁵(6.8), Ser⁷(6.2), Thr⁸(6.8), Asp¹¹(6.6), Ile¹⁶(5.6), Ile¹⁷(3.6), Asp¹⁸(3.4), Thr¹⁹(6.0), Val²⁰(4.7), Asn²¹(4.5), Phe²³(7.7), Thr²⁴(7.7), Lys²⁶(8.1); slow NH exchange, present after 12 h: Ile¹⁶, Ile¹⁷, Asp¹⁸, Thr¹⁹, Val²⁰, Thr²⁴, Lys²⁵, Lys²⁶, exchange < 12 h: Gln³, Ile⁵, Thr⁸, Ile⁹, Asn²¹, and possibly Asp⁴, Gly¹⁰ and Asp¹¹.

Ac-Pro¹⁴-δ-toxin 4a. Amino acid ratios: Met(1) 0.49, Ala(1) 0.98, Glu(1) 1.02, Asp(4) 4.17, Ile(5) 3.79, Ser(1) 0.86, Thr(3) 2.78, Gly(1) 1.00, Leu(1) 0.99, Val(2) 1.93, Pro(1) 0.98, Lys(3) 2.86, Phe(1) 1.00 (Found: MH⁺ 2989.61529. C₁₃₇H₂₂₃N₃₂O₄₀S⁺ requires *M*, 2989.61524).

Des-Lys¹⁴-δ-toxin 5. Amino acid ratios: Met(1) 0.91, Ala(1) 1.01, Glu(1) 1.02, Asp(4) 3.93, Ile(5) 3.98, Ser(1) 0.83, Thr(3) 2.72, Gly(1) 1.03, Leu(1) 1.00, Val(2) 1.94, Lys(3) 2.94, Phe(1) 1.00 (Found: MH⁺ 2850.55188. C₁₃₀H₂₁₄N₃₁O₃₈S⁺ requires *M*, 2850.55192) δ_H[c 1.1 mmol dm⁻³ in CD₃OH-H₂O (2:1); 600 MHz] Met¹: αCH(4.06), βCH₂(2.19, 2.16), γCH₂(2.63), εCH₃(2.13); Ala²: NH(8.80), αCH(4.35), βCH₃(1.44); Gln³: NH(8.55), αCH(4.26), βCH₂(2.07, 2.00), γCH₂(2.36), δNH₂(7.54, 6.83); Asp⁴: NH(8.48), αCH(4.67), βCH₂(2.90); Ile⁵: NH(8.15), αCH(4.08), βCH(1.95), γCH₂(n.a.), γCH₃(0.95^a), δCH₃(0.92^a); Ile⁶: NH(7.90), αCH(3.93), βCH(1.97), γCH₂(1.25), γCH₃(0.94^b), δCH₃(0.88^b); Ser⁷: NH(8.11), αCH(4.36), βCH₂(3.96, 3.87); Thr⁸: NH(7.95), αCH(4.16), βCH(4.34), γCH₃(1.25); Ile⁹: NH(8.23), αCH(3.85), βCH(1.96), γCH₂(1.25), γCH₃(0.94^c), δCH₃(0.88^c); Gly¹⁰: NH(8.35), αCH₂(3.93, 3.78); Asp¹¹: NH(8.21), αCH(4.64), βCH₂(3.14, 2.90); Leu¹²: NH(8.07),

αCH(4.16), βCH₂(1.90), γCH(1.77), δCH₃(0.96, 0.92); Val¹³: NH(8.33), αCH(3.53), βCH(2.20), γCH₃(1.07, 0.93); Trp¹⁵: NH(8.03), αCH(4.29), βCH₂(3.57, 3.37), 2H(7.17), 4H(7.56), 5H(7.02), 6H(7.13), 7H(7.40), NH(10.15); Ile¹⁶: NH(8.40), αCH(3.51), βCH(2.13), γCH₂(n.a.), γ,δCH₃(0.92); Ile¹⁷: NH(8.44), αCH(3.57), βCH(1.93), γCH₂(1.77), γCH₃(0.93^d), δCH₃(0.83^d); Asp¹⁸: NH(8.71), αCH(4.39), βCH₂(2.96, 2.69); Thr¹⁹: NH(7.99), αCH(3.77), βCH(4.00), γCH₃(0.97); Val²⁰: NH(8.36), αCH(3.72), βCH(2.17), γCH₃(1.02, 0.95); Asn²¹: NH(8.21), αCH(4.55), βCH₂(2.85, 2.74), γNH₂(7.63, 6.89); Lys²²: NH(7.80), αCH(4.00), βCH₂(1.75, 1.65), γCH₂(1.31, 1.14), δCH₂(1.54), εCH₂(2.83); Phe²³: NH(7.92), αCH(4.59), βCH₂(3.31, 3.03), 2, 6H(7.35^e), 3, 5H(7.30^e), 4H(7.25^e); Thr²⁴: NH(7.74), αCH(4.29), βCH(4.22), γCH₃(1.27); Lys²⁵: NH(8.09), αCH(4.29), βCH₂(1.88, 1.84), γCH₂(1.48), δCH₂(1.69), εCH₂(2.97); Lys²⁶: NH(8.22), αCH(4.37), βCH₂(1.92, 1.76), γCH₂(1.47), δCH₂(1.67), εCH₂(2.98), (^{a,b,c,d,e}these have not been unambiguously assigned and may be reversed); ³J_{NH-αCH}: Ala²(5.1), Gln³(5.6), Asp⁴(6.2), Ile⁵(5.2), Ser⁷(4.7), Thr⁸(4.4), Leu¹²(< 5.0), Trp¹⁵(< 5.0), Ile¹⁶(< 5.0), Ile¹⁷(< 5.0), Asp¹⁸(< 5.0), Thr¹⁹(4.4), Lys²²(3.8), Thr²⁴(7.6), Lys²⁶(7.0); slow NH exchange, present after 14 h: Val¹³, Trp¹⁵, Ile¹⁶, Ile¹⁷, Asp¹⁸, Thr¹⁹, exchange < 14 h: Ile⁹, Asp¹¹, Leu¹², Val²⁰, Asn²¹, Lys²², Phe²³ and Thr²⁴.

Ac-des-Lys¹⁴-δ-toxin 5a. Amino acid ratios: Met(1) 0.66, Ala(1) 1.03, Glu(1) 1.03, Asp(4) 4.11, Ile(5) 4.11, Ser(1) 0.65, Thr(3) 2.95, Gly(1) 0.98, Leu(1) 1.00, Val(2) 1.98, Lys(3) 2.79, Phe(1) 1.00 (Found: MH⁺ 2892.56260. C₁₃₂H₂₁₆N₃₁O₃₉S⁺ requires *M*, 2892.56248).

Glu⁸, Pro¹⁴-δ-toxin 6. Amino acid ratios: Met(1) 0.89, Ala(1) 0.95, Glu(2) 1.98, Asp(4) 3.77, Ile(5) 3.89, Ser(1) 0.79, Thr(2) 1.75, Gly(1) 0.98, Leu(1) 0.98, Val(2) 1.85, Pro(1) 0.96, Lys(3) 2.83, Phe(1) 1.00 (Found: MH⁺ 2975.59946. C₁₃₆H₂₂₁N₃₂O₄₀S⁺ requires *M*, 2975.59959) δ_H[c 1.9 mmol dm⁻³ in CD₃OH-H₂O (2:1); 600 MHz] Met¹: αCH(4.06), βCH₂(2.20, 2.16), γCH₂(2.64), εCH₃(2.13); Ala²: NH(8.78), αCH(4.37), βCH₃(1.43); Gln³: NH(8.45), αCH(4.33), βCH₂(2.10, 1.98), γCH₂(2.36), δNH₂(7.56, 6.84); Asp⁴: NH(8.43), αCH(4.72), βCH₂(2.90, 2.80); Ile⁵: NH(7.98), αCH(4.21), βCH(1.90), γCH₂(1.48, 1.20), γ,δ-CH₃(0.90); Ile⁶: NH(8.04), αCH(4.23), βCH(1.91), γCH₂(1.50, 1.20), γCH₃(0.92^a), δCH₃(0.87^a); Ser⁷: NH(8.11), αCH(4.46), βCH₂(3.83); Glu⁸: NH(8.13), αCH(4.38), βCH₂(2.00), γCH₂(2.43, 2.23); Ile⁹: NH(8.23), αCH(4.10), βCH(1.88), γCH₂(1.53, 1.26), γCH₃(0.95^b), δCH₃(0.90^b); Gly¹⁰: NH(8.63), αCH₂(3.89); Asp¹¹: NH(8.16), αCH(4.77), βCH₂(2.93, 2.88); Leu¹²: NH(8.21), αCH(4.44), βCH₂(1.79), γCH(1.73), δCH₃(0.95, 0.87); Val¹³: NH(8.00), αCH(3.95), βCH(2.21), γCH₃(1.06, 0.92); Pro¹⁴: αCH(4.19^{*}), βCH₂(2.25^{*c}, 2.09^{*c}), γCH₂(1.91^{*c}, 1.76^{*c}), δC-H₃(3.67^{*}); Trp¹⁵(1): NH(8.22), αCH(4.58), βCH₂(2.84, 2.78), [Trp¹⁵(2): NH(7.50), αCH(4.42), βCH₂(3.46, 3.36)], 2H(7.23), 4H(7.55), 5H(7.03), 6H(7.15), 7H(7.41), NH(10.25); Ile¹⁶: NH(8.17), αCH(3.66), βCH(2.03), γCH₂(n.a.), γ,δCH₃(0.88); Ile¹⁷: NH(8.11), αCH(3.70), βCH(1.92), γCH₂(1.66, 1.19), γCH₃(0.91), δCH₃(0.83); Asp¹⁸: NH(8.11), αCH(4.24), βCH₂(3.31, 3.06); Thr¹⁹: NH(7.92), αCH(3.94), βCH(4.15), γCH₃(1.10); Val²⁰: NH(8.21), αCH(3.80), βCH(2.18), γCH₃(1.02, 0.96); Asn²¹: NH(8.34), αCH(4.48), βCH₂(2.95, 2.82^{*}), γNH₂(7.62, 6.90); Lys²²: NH(7.92), αCH(4.05), βCH₂(2.74, 1.67), γCH₂(1.32, 1.19), δCH₂(1.56), εCH₂(2.85); Phe²³: NH(7.99), αCH(4.60), βCH₂(3.30, 3.04), 2,6H(7.34^d), 3,5H(7.30^d), 4-H(7.26^d); Thr²⁴: NH(7.75), αCH(4.31), βCH(4.25), γCH₃(1.27); Lys²⁵: NH(8.11), αCH(4.31), βCH₂(1.87, 1.83), γCH₂(1.49), δCH₂(1.70), εCH₂(2.98); Lys²⁶: NH(8.23), αCH(4.39), βCH₂(1.93, 1.77), γCH₂(1.47), δCH₂(1.68), εCH₂(2.98), (^{a,b,c,d}these have not been unambiguously assigned and may be reversed, ^{*}assigned from the NOESY spectrum, not observed in the TOCSY spectrum); ³J_{NH-αCH}: Ala²(5.6), Gln³(6.8), Asp⁴(7.3), Ile⁶(7.5), Gly¹⁰(5.3) and Thr²⁴(7.5).

Ac-Glu⁸, Pro¹⁴-δ-toxin 6a. Amino acid ratios: Met(1) 0.85,

Ala(1) 0.94, Glu(2) 2.04, Asp(4) 3.81, Ile(5) 3.90, Ser(1) 0.80, Thr(2) 1.73, Gly(1) 0.96, Leu(1) 0.98, Val(2) 1.87, Pro(1) 1.01, Lys(3) 2.85, Phe(1) 1.00 (Found: MH^+ 3017.61008. $C_{138}H_{223}N_{32}O_{41}S^+$ requires M , 3017.61015).

Glu⁷, des-Lys¹⁴- δ -toxin 7. Amino acid ratios: Met(1) 0.78, Ala(1) 0.91, Glu(2) 2.10, Asp(4) 3.93, Ile(5) 4.27, Thr(3) 2.63, Gly(1) 1.01, Leu(1) 1.09, Val(2) 1.99, Lys(3) 3.06, Phe(1) 1.00 (Found: MH^+ 2892.56260. $C_{132}H_{216}N_{31}O_{39}S^+$ requires M , 2892.56248).

Ac-Glu⁷, des-Lys¹⁴- δ -toxin 7a. Amino acid ratios: Met(1) 0.88, Ala(1) 0.97, Glu(2) 2.30, Asp(4) 3.98, Ile(5) 4.24, Thr(3) 2.70, Gly(1) 0.99, Leu(1) 1.06, Val(2) 1.94, Lys(3) 2.97, Phe(1) 1.00 (Found: MH^+ 2934.57299. $C_{134}H_{218}N_{31}O_{40}S^+$ requires M , 2934.57304).

Acknowledgements

The authors wish to thank Dr. D. W. Thomas for his invaluable help in processing the NMR spectra. We are also indebted to K. Shaw, B. Whigham and A. Taylor for expert technical assistance and to Professor R. Ramage for financial assistance. A referee is also acknowledged for very useful comments concerning the NMR studies.

References

- For some reviews see: G. Eisenman and J. A. Dani, *Ann. Rev. Biophys. Biophys. Chem.*, 1987, **16**, 205; W. A. Catterall, *Science*, 1988, **242**, 50; L. Y. Jan and Y. N. Jan, *Cell*, 1989, **56**, 13.
- M. Noda, T. Ikeda, T. Kayano, H. Suzuki, H. Takeshima, M. Kurasaki, H. Takahashi and S. Numa, *Nature*, 1986, **320**, 188.
- A. J. Yool and T. L. Schwarz, *Nature*, 1991, **349**, 700; G. Yellen, M. E. Jurman, T. Abramson and R. MacKinnon, *Science*, 1991, **251**, 939; H. A. Hartmann, G. E. Kirsch, J. A. Drewe, M. Tagliatalata, R. H. Joho and A. M. Brown, *Science*, 1991, **251**, 942.
- For recent reviews see: M. S. P. Sansom, *Prog. Biophys. Molec. Biol.*, 1991, **55**, 139; D. M. Ojcius and J. D.-E. Young, *Trends Biochem. Sci.*, 1991, **16**, 225.
- M. T. Tosteson and D. C. Tosteson, *Biophys. J.*, 1981, **36**, 109; M. T. Tosteson, O. Alvarez, W. Hubbell, R. M. Bieganski, C. Attenbach, L. H. Caporales, J. J. Levy, R. F. Nutt, M. Rosenblatt and D. C. Tosteson, *Biophys. J.*, 1990, **58**, 1367.
- R. O. Fox Jr. and F. M. Richards, *Nature*, 1982, **300**, 325.
- Y. Shai, J. Fox, C. Caratsch, Y.-L. Shih, C. Edwards and P. Lazarovici, *FEBS Lett.*, 1988, **242**, 161; Y. Shai, D. Bach and A. Yanovsky, *J. Biol. Chem.*, 1990, **265**, 20202.
- J. D. Lear, Z. R. Wassermann and W. F. DeGrado, *Science*, 1988, **240**, 1177; W. F. DeGrado and J. D. Lear, *Biopolymers*, 1990, **29**, 205.
- G. Spach, H. Duclouhier, G. Molle and J.-M. Valletton, *Biochimie*, 1989, **71**, 11.
- I. R. Mellor, D. H. Thomas and M. S. P. Sansom, *Biochim. Biophys. Acta*, 1988, **942**, 280.
- M. Noda, S. Shimizu, T. Tanabe, T. Takai, T. Kayano, T. Ikeda, H. Takahashi, H. Nakayama, Y. Kanaoka, N. Minamino, K. Kangawa, H. Matsuo, M. A. Raftery, T. Hirose, S. Inayama, H. Hayashida, T. Miyata and S. Numa, *Nature*, 1984, **312**, 121.
- A. Baumann, I. Krah-Jentgens, R. Muller, F. Muller-Holtkamp, R. Seidel, N. Kecskemethy, J. Casal, A. Ferrus and O. Pongs, *EMBO J.*, 1987, **6**, 3419; A. Wei, M. Covarrubias, A. Butler, K. Baker, M. Pak and L. Salkoff, *Science*, 1990, **248**, 599.
- T. McCormack, E. C. Vega-Saenz de Meira and B. Rudy, *Proc. Natl. Acad. Sci. USA*, 1990, **87**, 5227.
- T. Tanabe, H. Takeshima, A. Mikami, V. Flockerzi, H. Takahashi, K. Kangawa, M. Kojima, H. Matsuo, T. Hirose and S. Numa, *Nature*, 1987, **328**, 313.
- Y. Mori, T. Friedrich, M.-S. Kim, A. Mikami, J. Nakai, P. Ruth, E. Bosse, F. Hofmann, V. Flockerzi, T. Furuichi, K. Mikoshiba, K. Imoto, T. Tanabe and S. Numa, *Nature*, 1991, **350**, 398.
- D. N. Woolfson, R. J. Mortishire-Smith and D. H. Williams, *Biochem. Biophys. Res. Commun.*, 1991, **175**, 733.
- M. J. Tappin, A. Pastore, R. S. Norton, J. H. Freer and I. D. Campbell, *Biochemistry*, 1988, **27**, 1643.
- K. H. Lee, J. E. Fritton and K. Wüthrich, *Biochim. Biophys. Acta*, 1987, **911**, 144.
- K. Wüthrich, *NMR of Proteins and Nucleic Acids*, Wiley, New York, 1986.
- D. E. Blagdon and M. Goodman, *Biopolymers*, 1975, **14**, 241.
- J. M. Blaney, G. M. Crippen, A. Dearing and J. S. Dixon, QCPE Program 590.
- (a) A. Widmer, *QCPE Bulletin*, 1993, **13**, 2; (b) H. P. Lindner, *Tetrahedron*, 1974, **30**, 1127; (c) M. Sanner, A. Widmer, H. Senn and W. Braun, *J. Comput. Aided Molecular Design*, 1989, **3**, 195.
- P. Bladon and R. Breckenridge, *QCPE Bulletin*, 1993, **13**, 1.
- Ref. 19, p. 127.
- D. Eisenberg, J. U. Bowie, R. Luthy and S. Choe, *Faraday Discuss.*, 1992, **93**, 25.
- F. C. Bernstein, T. F. Koetzle, G. J. B. Williams, E. F. Meyer, Jr., M. D. Brice, J. R. Rodgers, O. Kennard, T. Shimanouchi and M. Tasumi, *J. Mol. Biol.*, 1977, **112**, 535.
- E. Atherton and R. C. Sheppard, *Solid Phase Peptide Synthesis*, IRL Press, Oxford, 1989.
- E. Kaiser, R. L. Colescott, C. D. Bossinger and P. I. Cook, *Anal. Biochem.*, 1970, **34**, 595.
- W. S. Hancock and J. E. Battersby, *Anal. Biochem.*, 1976, **71**, 260.
- S.-S. Wang, *J. Am. Chem. Soc.*, 1973, **95**, 1328.
- D. J. States, R. A. Haberkorn and D. J. Ruben, *J. Magn. Reson.*, 1982, **48**, 286.

Paper 3/00396E

Received 21st January 1993

Accepted 25th March 1993